# Variable Luminescence and Chromaticity of Homoleptic Frameworks of the Lanthanides together with Pyridylpyrazolates

Heba Youssef,[a, b] Alexander E. Sedykh,[a] Jonathan Becker,[a] Thomas Schäfer,[a] Ilya V. Taydakov,[c] Huanrong R. Li,[d] and Klaus Müller-Buschbaum*[a, e]

**Abstract:** Homoleptic, 3D coordination polymers of the formula $^{33}_{\infty}$[Ln(3-PyPz)$_3$] and $^{3}_{\infty}$[Ln(4-PyPz)$_3$], (3-PyPz)$^-$ = 3-(3-pyridyl)pyrazolate anion, (4-PyPz)$^-$ = 3-(4-pyridyl)pyrazolate anion, both C$_8$H$_6$N$_3^-$, Ln = Sm, Eu, Gd, Tb, Dy, were obtained as highly luminescent frameworks by reaction of the lanthanide metals (Ln) with the aromatic heterocyclic amine ligands 3-PyPzH and 4-PyPzH. The compounds form two isotypic series of 3D coordination polymers and exhibit fair thermal stability up to 360 °C. The luminescence properties of all ten compounds were determined in the solid state, with an antenna effect through ligand–metal energy transfer leading to high efficiency of the luminescence displayed by good quantum yields of up to 74 %. The emission is mainly based on ion-specific lanthanide-dependent intra 4f–4f transitions for Tb$^{3+}$: green, Dy$^{3+}$: yellow, Sm$^{3+}$: orange-red, Eu$^{3+}$: red. For the Gd$^{3+}$-containing compounds, the yellow emission of ligand triplet-based phosphorescence is observed at room temperature and 77 K. Co doping of the Gd-containing frameworks with Eu$^{3+}$ and Tb$^{3+}$ allow further shifting of the chromaticity towards white light emission.

## Introduction

During the past two decades, the hybrid nature of coordination polymers (CPs) and the related metal–organic frameworks (MOFs), composed of metal ions or clusters connected with organic linkers, has been the focus of many research efforts.[1] They give rise to properties derived from either one of the two components or the combination of both. The hybrid material can thereby generate cooperative properties, such as porosity,[2] magnetism,[3] photoluminescence (PL),[4] or nonlinear optical properties.[5]

Lanthanide-based hybrid compounds are important chromophores for lighting, displays, and lasers, giving characteristic narrow line emissions, whereas they have intrinsically low absorption coefficients as a result of the parity-forbidden 4f–4f transitions.[6] Consequently, an antenna such as an organic molecule promotes light harvesting by absorption of photon energy, usually in a broad UV range, and transfer it intramolecularly to the Ln$^{3+}$ ion thereby enhance the efficiency of emission.[7] The direct coordination of a conjugated π-electron system to the metal ions could act as a good sensitizer. However, the ion has to be shielded from vibronic quenchers, for instance, deactivating solvents such as water, as these allow quenching of the elevated state of the Ln$^{3+}$-ions due to vibronic deactivation.[8] Numerous efforts have been made to enlarge the absorption coefficients and thus obtain significantly more intense lanthanide ion emissions.[9] In addition, the generation of white light by mixing different monochromatic light sources is an attractive feature of light-emitting materials recently.[10]

The ligand 3-(3-pyridyl)pyrazole (3-PyPzH) was used mainly as a reactant in ligand synthesis, and some of those new derivative ligands were used later in coordination chemistry.[11] The ligand 3-(4-pyridyl)pyrazole (4-PyPzH) has been mainly applied in the synthesis of transition metal-based complexes and CPs. For instance, two Hofmann-like 2D coordination polymers with the general formula of {Fe$^{2+}$(Hppy)$_2$[M$^{2+}$(CN)$_4$]·H$_2$O, (M = Pd, Pt), are known. Both compounds show two-step spin-crossover behavior with hysteresis loops around 14–

[a] H. Youssef, A. E. Sedykh, Dr. J. Becker, T. Schäfer, Prof. Dr. K. Müller-Buschbaum
Institute of Inorganic and Analytical Chemistry
Justus-Liebig-University Giessen
Heinrich-Buff-Ring 17, 35392 Giessen (Germany)
E-mail: klaus.mueller-buschbaum@anorg.chemie.uni-giessen.de

[b] H. Youssef
Department of Chemistry
Faculty of Science, Mansoura University
El Gomhouria, Mansoura Qism 2, Dakahlia Governorate, 11432, Mansoura (Egypt)

[c] Prof. Dr. I. V. Taydakov
Lebedev Physical Institute of the Russian Academy of Sciences
Leninskiy pr-t, 53, 119991, Moscow (Russia)

[d] Prof. Dr. H. R. Li
Hebei University of Technology
Guanrong Dao 8, Hongqiao District, 300130, Tianjin (P. R. China)

[e] Prof. Dr. K. Müller-Buschbaum
Center of Materials Research (LAMA)
Justus-Liebig-University Giessen
Heinrich-Buff-Ring 16, 35392 Giessen (Germany)

23 K.[12] This ligand was also used in the synthesis of a series of inorganic–organic hybrid materials based on polyoxometalates (POMs), $[M(HL)_2(H_2O)_2][Mo_6O_{20}]$ [M=Co, Ni, Cu, Zn], $[MnL_2(H_2O)_2][Mo_6O_{20}]$ and $(HL)_3PMo_{12}O_{40}$, with antiferromagnetic behavior.[13] 4-PyPzH was also used to prepare a $Cu^{2+}$ containing discrete metal complex gelator able to gel dimethylformamide (DMF) at 0.51 wt%.[14] Both ligands were used to produce highly efficient phosphorescent $Cu^+$ and $Ag^+$ complexes.[15] To the best of our knowledge, no lanthanide-containing compounds with these ligands have been known.
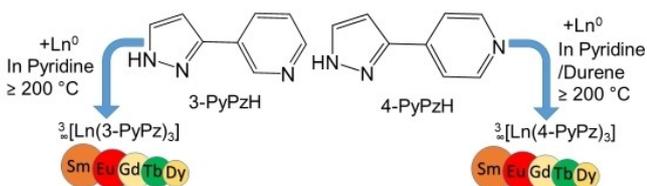
Based on these results, we were prompted to construct novel lanthanide coordination polymers and succeeded in the synthesis of frameworks featuring either 3-(3-pyridyl)pyrazole or 3-(4-pyridyl)pyrazole (3-PyPzH or 4-PyPzH). Herein, we report the synthesis, characterization, luminescence, and thermal properties of the homoleptic and co-doped frameworks $^3_\infty$[Ln-(3-PyPz)$_3$] and $^3_\infty$[Ln(4-PyPz)$_3$].

## Results and Discussion
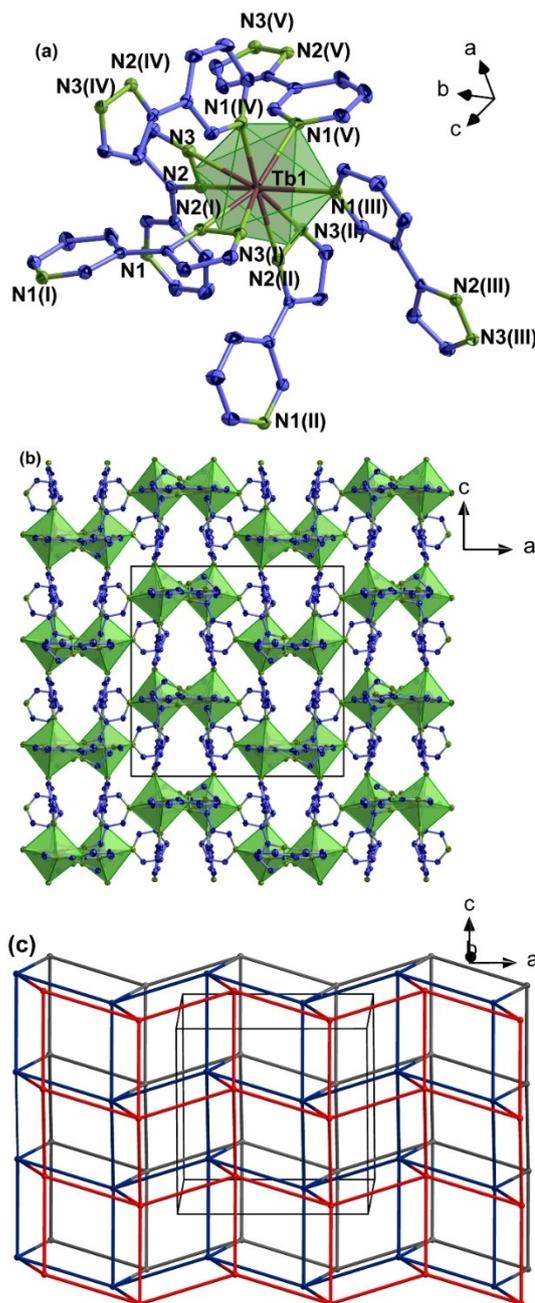
### Synthesis and structural analysis

The two series of ten coordination polymers $^3_\infty$[Ln(3-PyPz)$_3$] and $^3_\infty$[Ln(4-PyPz)$_3$] are formed in reactions of the elemental lanthanides with 3-(3-pyridyl)pyrazole (3-PyPzH) or 3-(4-pyridyl)pyrazole (4-PyPzH) (Scheme 1) in either pyridine or 1,2,4,5-tetramethyl-benzene (durene) with high yield (82–96%).

The homoleptic frameworks of the formula $^3_\infty$[Ln(3-PyPz)$_3$] (Ln = Sm, Eu, Gd, Tb, and Dy) (**1–5**, respectively) are isotypic and crystallize in the cubic space group $Pa\bar{3}$. The second isotypic coordination polymer series $^3_\infty$[Ln(4-PyPz)$_3$] (Ln = Sm, Eu, Gd, Tb, and Dy; **6–10**, respectively) is also formed of isotypic compounds that crystallize in the monoclinic crystal system in the space group $P2_1/n$. The $^3_\infty$[Ln(3-PyPz)$_3$] and $^3_\infty$[Ln(4-PyPz)$_3$] series constitute of three perspective pyridyl-pyrazolate anions per formula unit, resulting in the identical general chemical formula of $C_{24}H_{18}N_9Ln$. Each ligand acts as a tridentate ligand and forms a bridge between two neighboring trivalent lanthanide ions (Figures 1 and 2).[16] In sum, each $Ln^{3+}$ ion coordinates to nine N atoms in a pseudo-octahedral fashion, in which the two nitrogen atoms of the pyrazolate anion are regarded as a single connection and therefore as one corner of the octahedron. The topology was determined for **4** and **9** as a representative example for the two isotypic series to ensure a better understanding of the crystal structure. It was determined
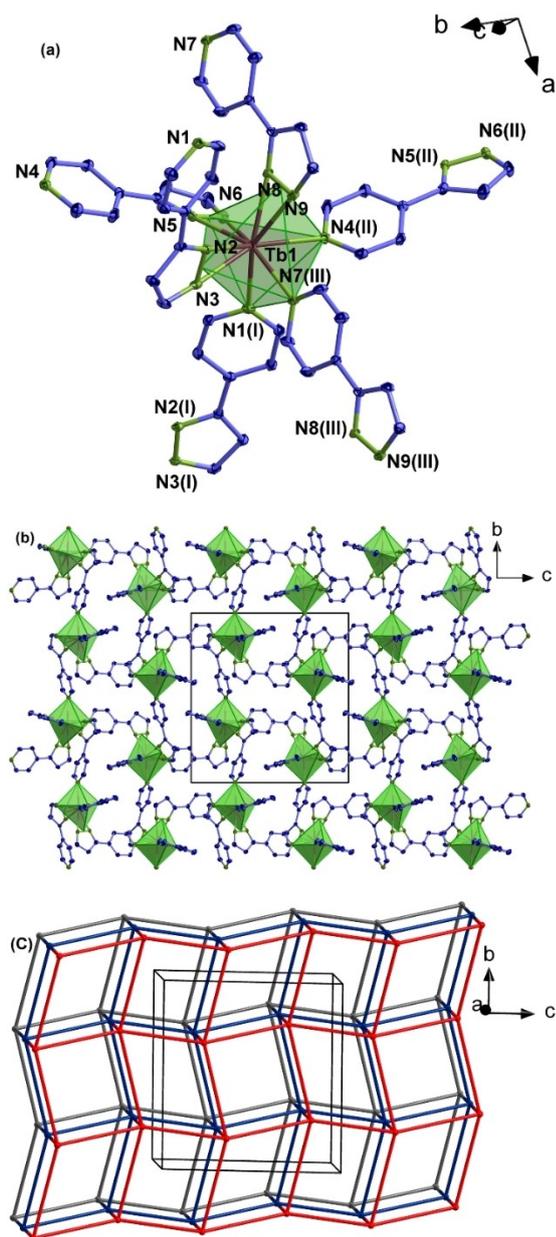


**Figure 1.** a) Extended coordination sphere of $Ln^{3+}$ in $^3_\infty$[Tb(3-PyPzH)$_3$] (**4**) representing the series of isotypic framework compounds (**1–5**). b) Crystal structure of **4** with a view along [010]. Hydrogen atoms are omitted for clarity. $Tb^{3+}$ ions are shown in brown, nitrogen atoms in green, carbon atoms in blue, and the coordination polyhedra around $Tb^{3+}$ are indicated in green with thermal ellipsoids depicted at the 50% probability level. c) Topological representation of **4** as a uninodal 6-c net with **pcu** topology. Symmetry operations: I = −z+1,x+1/2,−y+3/2, II = y−1/2,−z+3/2,−x+1, III = x−1/2,y,−z+3/2, IV = y−1/2,z,−x+3/2 V = z−1/2,x,−y+3/2.



**Scheme 1.** Synthetic scheme for two novel series of 3D coordination polymers with 3-PyPzH (left) and 4-PyPzH (right) ligands.

in conformity with the Reticular Chemistry Structure Resource (RCSR) and the Wells terminology.[17] Both structures of **4** and **9** indicate that there is a 6-connected uninodal net with a Schläfli symbol of $4^{12}.6^3$ (**pcu**; 6/4/c1; sqc1) when assuming that the terbium centers act as nodes with threefold connectivity.

**Chemistry–A European Journal**

**Full Paper**
doi.org/10.1002/chem.202103068

**Chemistry Europe**
European Chemical
Societies Publishing

**Figure 2.** a) Extended coordination sphere of Ln$^{3+}$ in $^3_\infty$[Tb(4-PyPzH)$_3$] (**9**) representing the series of isotypic framework compounds (**6–10**). b) Crystal structure of **9** with a view along [100]. Hydrogen atoms are omitted for clarity. Tb$^{3+}$ ions are shown in brown, nitrogen atoms in green, carbon atoms in blue, and the coordination polyhedra around Tb$^{3+}$ are indicated in green with thermal ellipsoids depicted at the 50% probability level. c) Topological representation of **9** as a uninodal 6-c net with **pcu** topology. Symmetry operations: I = x + 1/2, −y + 1/2, z + 1/2, II = −x + 3/2, y − 1/2, −z + 3/2, III = x + 1, y, z.

Although the packing of nets in **4** and **9** differs, the connectivity of all nodes is the same, which leads to the same underlying network topology. This results in 3D framework structures, in which six ligands act as bridges between the adjacent lanthanide ions.

The average distances between the metal ions and the pyridine nitrogen atoms (Tables S3 and S4 in the Supporting Information; 258(2) pm) in **1–10** are longer than the Ln–N

distances to the pyrazolate ring atoms (242(2) pm). This can be explained by the ionic character of the pyrazolate N sites compared to the neutral pyridyl donor.
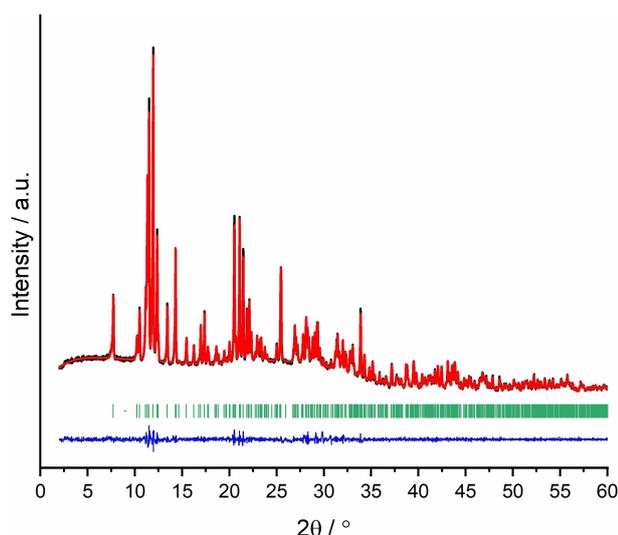
For the frameworks **1–5**, comparison and analysis of the lattice parameters indicates that the volume of the unit cell and the Ln–N1 distances as well as an average value of the Ln–N2 and Ln–N3 distances have a decreasing trend for an increase of charge density from samarium to dysprosium. The same behavior is observed for the second series of frameworks **6–10**, the average of Ln–N1, Ln–N4, and Ln–N7 (pyridine ring) as well as the average value of Ln–N2, Ln–N3, Ln–N5, Ln–N6, Ln–N8, and Ln–N9 (pyrazolate rings) decreasing from Sm$^{3+}$ to Dy$^{3+}$. Compound **4** cannot contribute to this, because the single-crystal X-ray measurement had to be performed at a different temperature of 200 K. At lower temperatures, the crystals cracked continuously.

Besides, the described phenomena are a direct consequence of lanthanide contraction.[18] For polymers, **6–10** partially occupied and heavily disordered pyridine solvent was found in voids in the crystal structure. For additional details on the crystal structure determinations of $^3_\infty$[Ln(3-PyPz)$_3$] and $^3_\infty$[Ln(4-PyPz)$_3$], see Tables S1 and S2; for selected interatomic distances and angles, see Tables S3, and S4, respectively.

All bulk products of the polymers (**1–10**) were proven to be phase pure bulk products by PXRD. The experimental diffraction patterns match well in terms of reflection positions and intensities with the diffraction patterns simulated from single-crystal data of compounds (**1–5**). No additional reflections of crystalline byproducts are observed, as shown in Figure 3 for **1** as a representative (for **2–5**, see also Figures S1–S4). To take the different measurement conditions of PXRD (298 K) and SCXRD (100 K) into account, additional Pawley-refinements for **6–10**, were carried out, confirming the phase purity of the respective series of coordination polymers. The resulting difference plots show no significant deviations as depicted in Figure 4 for **6** (see
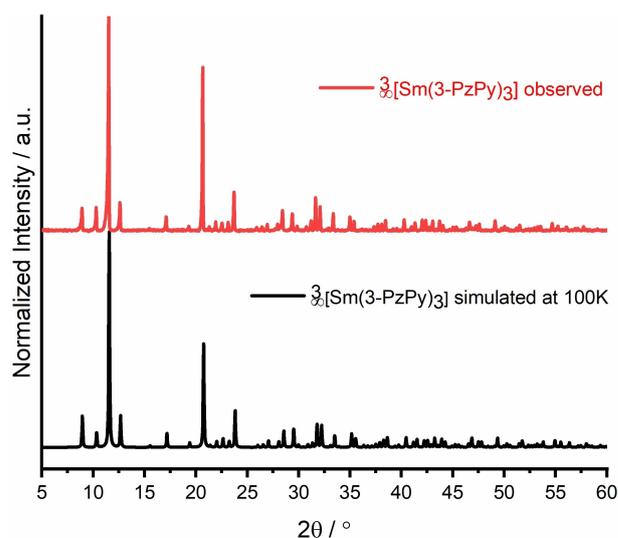


**Figure 3.** Comparison of the experimental X-ray powder diffraction pattern at 298 K (top) with a simulated pattern from single-crystal X-ray data of $^3_\infty$[Sm(3-PyPz)$_3$] (**1**) at 100 K (bottom).

**Chemistry–A European Journal**

Full Paper
doi.org/10.1002/chem.202103068

**Chemistry
Europe**
European Chemical
Societies Publishing

**Figure 4.** Pawley refinement results for PXRD of $^3_\infty$[Sm(4-PyPz)$_3$] (**6**), showing the experimental data (black) together with the Pawley fit (red), the corresponding difference plot (blue) as well as *hkl* position markers (green).

also Figures S5–S8). The details of the Pawley-refinements are listed in the Supporting Information, Table S5.

## Photophysical properties

The compounds of both series of homoleptic frameworks show photoluminescence properties for the range of investigated lanthanides. Excitation and emission spectra were recorded in the solid state at room temperature (RT = 298 K) and 77 K for the free ligands 3-PyPzH and 4-PyPzH,[14–15] as well as for the ten 3D coordination polymers $^3_\infty$[Ln(3-PyPz)$_3$] and $^3_\infty$[Ln(4-PyPz)$_3$], Ln = Sm, Eu, Tb, and Dy, and co-doped $^3_\infty$[Gd(3-PyPz)$_3$]: Eu$^{3+}$,Tb$^{3+}$ and $^3_\infty$[Gd(4-PyPz)$_3$]:Eu$^{3+}$,Tb$^{3+}$.

The investigated compounds (Figures 5 and 6) show a broad excitation band dominant in the UV with maxima at 312–320 nm for **1**–**10** at 77 K, which refers to ligand-based excitation, 330 nm for 3-PyPzH, and 370 nm for 4-PyPzH.

At RT (Figures S9–S20), the excitation maxima appear for **4** at 312 nm, for **1**, **3**, **5**, **6**, **8**, **9**, and **10** at 319–326 nm, and for the free ligands at about 333 nm. Excluding compounds containing Gd$^{3+}$ (**3** and **8**) and Eu$^{3+}$ (**2** and **7**), at RT, direct and weak excitation of the spin forbidden (Laporte selection rule),[19] 4f–4f transitions are also observed at both temperatures for the highlighted frameworks.
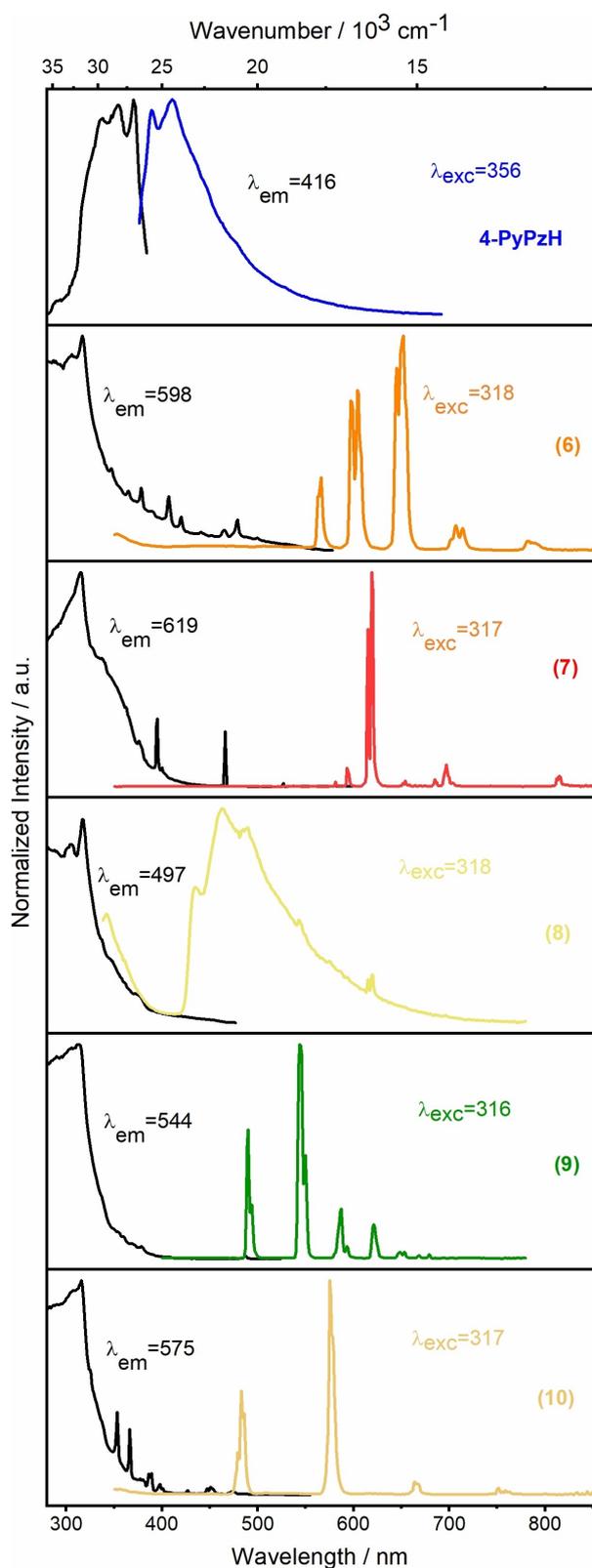
For the Eu$^{3+}$ containing compounds **2** and **7**, at RT, the spin-forbidden 4f–4f transitions are dominant in the excitation spectra, where the direct f-f excitation $^5D_2 \leftarrow {}^7F_0$ has the maximum intensity.

The synthesized compounds exhibit emission colors visible to the naked eye under the UV lamp which covers the primary RGB regions from blue (3-PyPzH, 4-PyPzH), green (Tb$^{3+}$ in **4**, **9**), to yellow-white (co-dopped Gd$^{3+}$ in **3**, **8**), through orange (Sm$^{3+}$ in **1**, **6**) to red (Eu$^{3+}$ in **2**, **7**). For 3-PyPzH and 4-PyPzH,
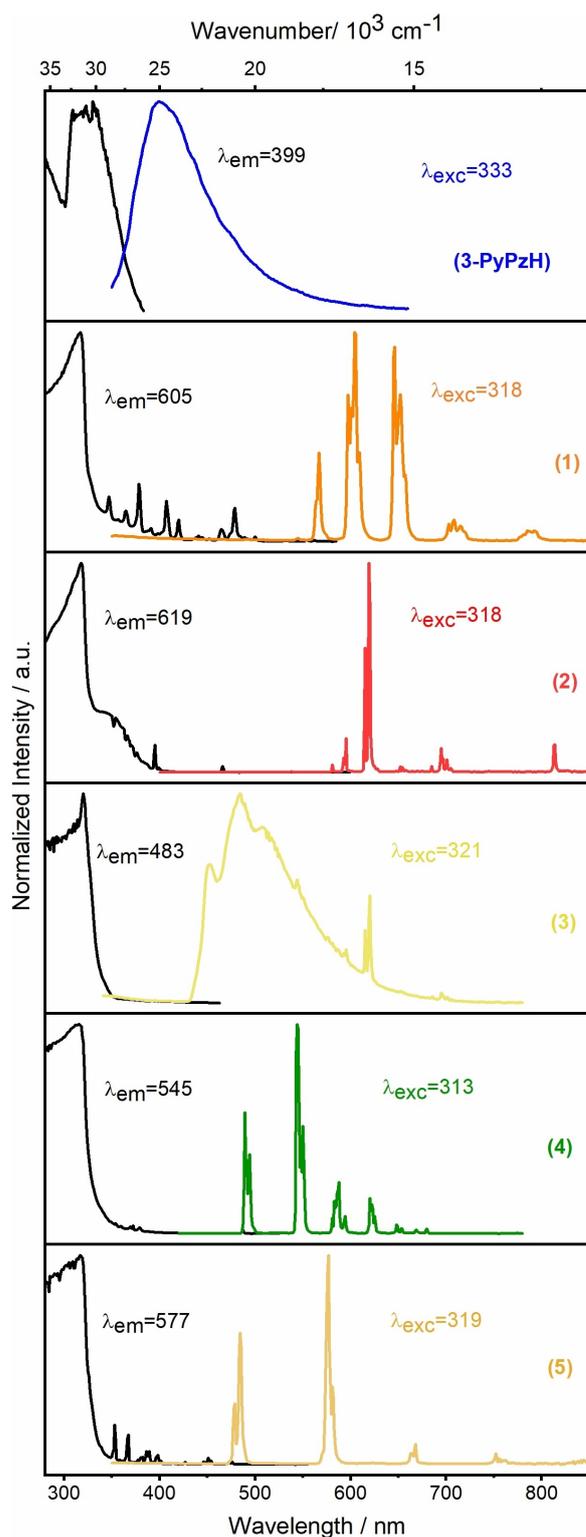


**Figure 5.** Normalized solid-state excitation (black) and emission (colored) spectra of $^3_\infty$[Ln(3-PyPz)$_3$], Ln = Sm, Eu, Gd, Tb, Dy (**1**–**5**) at 77 K. Wavelengths for which the spectra were recorded are reported in the legends.

the emission maxima appear in the range of 400 to 410 nm.[15] The emission profiles of Sm$^{3+}$ **1** and **6** display the characteristic transitions $^4G_{5/2} \rightarrow {}^6H_J$, $J = 5/2$–13/2 for Sm$^{3+}$ with the $^4G_{5/2} \rightarrow {}^6H_{7/2}$

**Chemistry–A European Journal**

Full Paper
doi.org/10.1002/chem.202103068

**Chemistry Europe**
European Chemical
Societies Publishing

**Figure 6.** Normalized solid-state excitation (black) and emission (colored) spectra of $^{3}_{\infty}[Ln(4\text{-PyPz})_3]$, Ln = Sm, Eu, Gd, Tb, Dy (**6–10**) at 77 K. Wavelengths for which the spectra were recorded are reported in the legends.

transition at 605 nm dominating the spectrum for **1**, while the hypersensitive $^4G_{5/2}\rightarrow{}^6H_{9/2}$ transition at 652 nm dominating the spectrum for **6** at 77 K. At RT, the transition to $^6H_{9/2}$ is dominating for **1** and **6**. At both temperatures, the red luminescence of $Eu^{3+}$ (**2** and **7**) is a result of transitions from its $^5D_0$ state to the $^7F_J$, $J=0$–6, levels related to the typical red emission of $Eu^{3+}$. In the emission spectra of both compounds, the hypersensitive $^5D_0\rightarrow{}^7F_2$ transition has the maximum intensity at 619 nm. In addition, transitions from a higher-level $^5D_1\rightarrow{}^7F_1$ at 537 (**2**), 538 nm (**7**), and $^5D_1\rightarrow{}^7F_2$ at 555 nm are observed. The transition $^5D_0\rightarrow{}^7F_0$ is an indication that the $Eu^{3+}$ ion occupies a site belonging to the $C_{nv}$, $C_n$, or $C_s$ class of symmetry[20] (in this particular case $C_3$), to evade the selection rules described by the Judd-Ofelt theory.

The terbium containing coordination polymers **4** and **9** show the typical emission transitions between the excited $^5D_4$ state and the $^7F_J$ ($J=6$–0) levels of $Tb^{3+}$. The characteristic $^5D_4\rightarrow{}^7F_J$, $J=3$–6, transitions result in bright green photoluminescence color. The highest intensity is found for the transition $^5D_4\rightarrow{}^7F_5$ at 543 and 544 nm for **4** and **9**, respectively, as expected for a $Tb^{3+}$.[1c]

For $^{3}_{\infty}[Dy(3\text{-PyPz})_3]$ (**5**) and $^{3}_{\infty}[Dy(4\text{-PyPz})_3]$ (**10**), four emission lines are observed corresponding to the transition from the first excited $^4F_{9/2}$ state to the states $^6H_{15/2}$, $^6H_{13/2}$, $^6H_{11/2}$, and $^6H_{9/2}$. The highest intensity band at 575 nm is attributed to the $^4F_{9/2}\rightarrow{}^6H_{13/2}$ transition.

The heavy paramagnetic $Gd^{III}$ ion in **3** and **8** enhances the inter-system crossing from the singlet to the triplet state of the pyrazolate anion.[21] Thus, it is feasible to obtain an evaluation of the $T_1$ energy level of both ligands by analyzing the emission spectra of $^{3}_{\infty}[Gd(3\text{-PyPz})_3]$ and $^{3}_{\infty}[Gd(4\text{-PyPz})_3]$, which is already visible at room temperature and more intense and better resolved at 77 K. The phosphorescent emission was also detected with a gating (cutting off the emission of the singlet state) to ensure a precise determination of the energetic positions of the $T_1$ level for the anions 3-PyPz$^-$ ($\lambda_{onset}=430$ nm, $\sim23\,250$ cm$^{-1}$; Figure S13) and 4-PyPz$^-$ ($\lambda_{onset}=423$ nm, $\sim23\,640$ cm$^{-1}$; Figure S18) at 77 K.[22] The emission spectra of the $Gd^{3+}$ samples also show characteristic $Eu^{3+}$ and $Tb^{3+}$ 4f–4f transitions indicating a small Eu and Tb-impurity relevant for photoluminescence. The low concentration of $Eu^{3+}$ and $Tb^{3+}$ ions in the structure lowers the probability of cross-relaxation, thus enhancing its metal center-based luminescence. Besides, the ligands are themselves good sensitizers for $Eu^{3+}$ and $Tb^{3+}$. The emission bands of $^{3}_{\infty}[Gd(3\text{-PyPz})_3]$:$Eu^{3+}$,$Tb^{3+}$ (**3**) are observable at 544, 620 and 695 nm at 77 K and assigned to $^5D_4\rightarrow{}^7F_5$ transition of $Tb^{3+}$, $^5D_0\rightarrow{}^7F_2$ and $^5D_0\rightarrow{}^7F_4$ transitions of $Eu^{3+}$, respectively. Characteristic for $Eu^{3+}$, the band at 615 nm correlates with the transition $^5D_0\rightarrow{}^7F_6$. It is also observable at RT, where the $^5D_0\rightarrow{}^7F_2$ transition is dominating the spectrum for $\lambda_{ex}=323$ nm. At 77 K, the emission spectrum of $^{3}_{\infty}[Gd(4\text{-PyPz})_3]$:$Eu^{3+}$,$Tb^{3+}$ (**8**) shows emission bands at 544 and 619 nm corresponding again to the $^5D_4\rightarrow{}^7F_5$ transition of $Tb^{3+}$ and $^5D_0\rightarrow{}^7F_2$ transition of $Eu^{3+}$. At RT, the characteristic band for $Tb^{3+}$ at 491 nm corresponding to the $^5D_4\rightarrow{}^7F_6$ transition appears, where the $^5D_4\rightarrow{}^7F_5$ transition is dominating the spectrum at $\lambda_{ex}=321$ nm. Besides, the transitions $^5D_0\rightarrow{}^7F_{3,4}$ of

**Chemistry–A European Journal**

**Full Paper**
doi.org/10.1002/chem.202103068

**Chemistry Europe**
European Chemical
Societies Publishing

$Eu^{3+}$ at 654, and 699 nm are observable. For both cases, **3** and **8**, a deliberate co-doping of the Gd-containing frameworks with $Tb^{3+}$ and $Eu^{3+}$ can be established and used for chromaticity tuning. Mixing of the three emission colors results in a shift towards yellow, orange,[23] and even towards the white point with color coordinates of $x = 0.30$ and $y = 0.37$ for 0.5% Eu (**3b**) at 77 K. The possibility of tuning the luminescence chromaticity by co-doping of other homoleptic frameworks was also investigated and verified (Figures S24 and S25) for the co-doping of the Tb- and Eu-containing frameworks (**2** and **4**) with the respective counterions. The experiments were carried out for 5%Tb to 95% Eu and *vice versa* to produce $^3_\infty[Eu_{0.95}Tb_{0.05}(3\text{-}PyPz)_3]$ (**2a**), and $^3_\infty[Tb_{0.95}Eu_{0.05}(3\text{-}PyPz)_3]$ (**4a**), respectively. In both cases, the emission spectra of **2a** and **4a** are dominated by the main metal ion. In addition, a slight downshift metal-to-metal energy transfer (MMET) from excited 4f states of $Tb^{3+}$ to $Eu^{3+}$ is observed. The emission colors of $^3_\infty[Gd_{1\text{-}x\text{-}y}Eu_xTb_y(3\text{-}PyPz)_3]\text{:}Eu^{3+},Tb^{3+}$ (**3a–3f**), $^3_\infty[Gd_{1\text{-}x\text{-}y}Eu_xTb_y(4\text{-}PyPz)_3]\text{:}Eu^{3+},Tb^{3+}$ (**8a–8f**), $^3_\infty[Eu_{0.95}Tb_{0.05}(3\text{-}PyPz)_3]$ (**2a**) and $^3_\infty[Tb_{0.95}Eu_{0.05}(3\text{-}PyPz)_3]$ (**4a**) are illustrated in CIE 1931 chromaticity diagrams (Figures 7 and S26), and the color coordinates are listed in Table S7. Excitation and emission spectra for the deliberate doping experiments are depicted in Figures S21–S25.

$$\phi_{calc} = \frac{\tau_{obs}}{\tau_0}$$

Neither a significant ligand-based fluorescence nor phosphorescence is being observed for the described coordination polymers except for $Gd^{3+}$. Thus 3-PyPz⁻ and 4-PyPz⁻ act as a suitable antenna for the sensitization of the lanthanide-based emission through absorption of light by the ligand by an $S_n \leftarrow S_0$ transition, ISC (intersystem crossing) from singlet (S) to triplet $(T_1)$ levels of the ligands, followed by an energy transfer to the lanthanide ions, which then emit from their excited 4f states.

Lifetime measurements by determination of the overall process decay time were performed for all the compounds at room temperature and 77 K. In addition, quantum yields (QY) were determined if possible to further quantify the luminescence properties in the visible region supporting the discussion of transitions. The lifetimes were determined for $Sm^{3+}$ (about 0.016 ms for **1** and **6**) and $Dy^{3+}$ (0.016 for **6**, and 0.012 ms for **10**) as well as for $Tb^{3+}$ (1.0874 ms for **4**, and 0.6273 ms for **9**; Table 1).

The PL of the coordination polymers decays monoexponentially on the timescale of a few milliseconds, thus indicating the presence of a single emissive species except for the co-doped $Gd^{3+}$ frameworks. The lifetime for $^3_\infty[Gd(3\text{-}PyPz)_3]\text{:}Eu^{3+},Tb^{3+}$ (**3**) and $^3_\infty[Gd(4\text{-}PyPz)_3]\text{:}Eu^{3+},Tb^{3+}$ (**8**) at 77 K were fitted biexponentially, $\tau_1 = 1.55$ ms, $\tau_2 = 5.03$ ms for **3** and $\tau_1 = 0.35$ ms, $\tau_2 = 1.43$ ms for **8**, corroborating the observation of more than one PL process. The lifetime of the co-doped frameworks **3a–3f**, **8a–8f**, **2a**, and **4a** are varying from 0.516–0.750 ms at RT (Table S8). For most of the samples, the lifetime at 77 K rises slightly, as the thermal quenching of luminescence decreases.

The observed quantum yield (QY) for the $Ln^{3+}$ emission through an antenna effect excitation (Table 1) is found to be
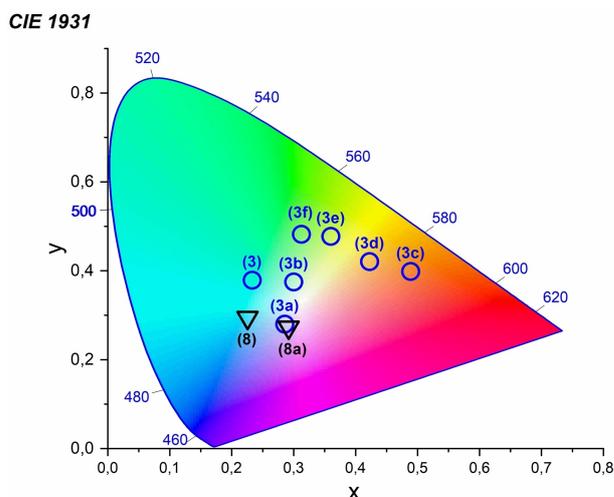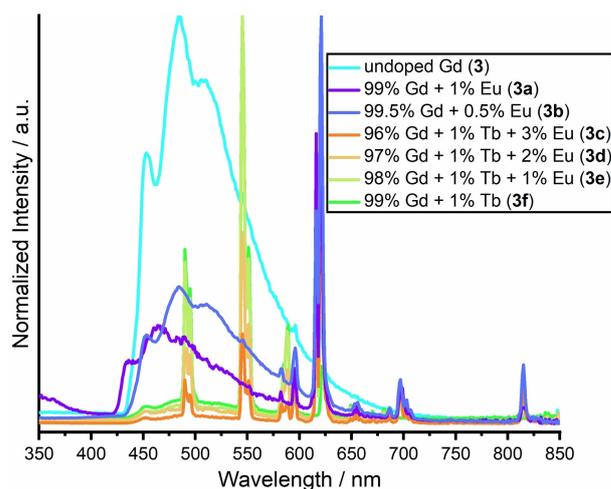


*CIE 1931*



**Figure 7.** Normalized emission spectra of $^3_\infty[Gd_{1\text{-}x\text{-}y}Eu_xTb_y(3\text{-}PyPz)_3]\text{:}$ $Eu^{3+},Tb^{3+}$ (**3a–3f**) at 77 K (top), $\lambda_{ex} = 323$ nm. Chromaticity coordinate diagram (CIE 1931) of the emission colors of the series $^3_\infty[Gd_{1\text{-}x\text{-}y}Eu_xTb_y(3\text{-}PyPz)_3]\text{:}Eu^{3+},Tb^{3+}$ (**3**, **3a–3f**) and $^3_\infty[Gd_{1\text{-}x\text{-}y}Eu_xTb_y(4\text{-}PyPz)_3]\text{:}Eu^{3+},Tb^{3+}$ (**8**, **8a**) at 77 K.

highest for the $Tb^{3+}$ compounds (**4** and **9**) with QY = 74(1) and 23(1) %, respectively. This is a result of energy gaps in the optimal range (2500–3000 cm⁻¹) for **4** ($\Delta E = \sim 2756$ cm⁻¹) and slightly above the optimal value for **9** ($\Delta E = \sim 3141$ cm⁻¹), indicating an excellent antenna effect especially for **4**. The measured QY for $Sm^{3+}$ is less than 1% and less than the calculated one ($\Phi_{calc} = 6.15\%$) which was determined using Equation (1), where $\tau_{obs}$ (0.016 ms) is the measured radiative lifetime and $\tau_o$ (3.25 ms) is the calculated average natural lifetime of $Sm^{3+}$.[24] Altogether, it is in the range of other known compounds containing $Sm^{3+}$.[22,24c,25] The quantum efficiencies for the Dy-containing frameworks **5** and **10** were determined as 1%, which is also in the range of other $Dy^{3+}$ compounds.[26]

The internal quantum yields (IQY) of the $Eu^{3+}$ centered emission were calculated using the following Wert's formula, see Equation (2).[27] $A_{MD,0} = 14.65$ S⁻¹ for $Eu^{3+}$, which represents the constant spontaneous emission probability, $I_{tot}$ represents the total area of the emission spectrum ($^5D_0 \rightarrow {}^7F_J$, $J = 0$–6), and

Chemistry–A European Journal | Full Paper
doi.org/10.1002/chem.202103068

**Chemistry**
**Europe**
European Chemical
Societies Publishing

**Table 1.** Photophysical data of 3-PyPzH, 4-PyPzH, and **1–10** in the solid-state at room temperature and 77 K.

| ID | $\tau$[a] [ms] | $\lambda_{ex}/\lambda_{em}$ [nm][b] | $\tau$[c] [ms] | $\lambda_{ex}/\lambda_{em}$ [nm][d] | $\Phi$ [%][e] | $\lambda_{ex}/\lambda_{em}$ [nm][f] |
|---|---|---|---|---|---|---|
| 3-PyPzH | 3.4(1) ns | 287/420 | 4.4(2) ns | 287/420 | n/a | n/a |
| 4-PyPzH | 6.07(9) ns | 287/420 | 6.80(7) ns | 287/420 | n/a | n/a |
| **1** | 0.01589(3) | 324/605 | 0.02043(1) | 318/605 | 0.46(1) | 321/550–770 |
| **2** | 0.576(1) | 466/619 | 0.754(2) | 318/619 | 0.33(3) | 363/570–715 |
| **3** | 0.5735(3) | 323/545 | 3.29(6) | 323/545 | n/a | n/a |
| **4** | 1.0874(8) | 313/545 | 1.060(2) | 314/545 | 74.3(2.2) | 322/475–685 |
| **5** | 0.01573(5) | 324/575 | 0.01587(7) | 319/484 | 1.13(4) | 321/460–675 |
| **6** | 0.01583(6) | 327/646 | 0.01739(7) | 318/598 | 0.40(1) | 324/545–735 |
| **7** | 0.323(1) | 466/619 | 0.498(1) | 317/619 | 0.11(1) | 330/570–715 |
| **8** | 0.56(1) | 321/545 | 0.885(2) | 314/545 | n/a | n/a |
| **9** | 0.6273(8) | 323/544 | 0.6089(8) | 316/544 | 23.2(3) | 320/475–690 |
| **10** | 0.01207(2) | 322/575 | 0.01270(3) | 317/575 | 1.15(3) | 321/460–675 |

[a] Emission lifetimes determined at 298 K. [b] Excitation and emission wavelengths for emission lifetime at 298 K. [c] Emission lifetime determined at 77 K. [d] Excitation and emission wavelengths for emission lifetime at 77 K. [e] Quantum yield. [f] Excitation wavelength and emission range of QY measurements.

$I_{MD,0}$ is the area of the $^5D_0 \rightarrow {}^7F_1$ transition. According to the literature,[28] the refractive index equals 1.5, $\tau_{rad} = 1.187$ and 0.988 ms, and $\tau_{obs} = 0.576(1)$ and 0.016(6) for compounds **2** and **7**, respectively. The equation gives a moderate-high Internal QY (Eu$^{3+}$) of 48 and 33% for **2** and **7**, respectively.

$$IQY = \frac{\tau_{obs}}{\tau_{rad}} = \tau_{obs} A_{MD,0} n^3 \left( \frac{I_{tot}}{I_{MD}} \right) \qquad (2)$$

**Thermal analysis**

Simultaneous DTA and TG investigations for $^3_\infty[\text{Tb(3-PyPz)}_3]$ (**4**), as well as DTA/TG, combined with mass spectrometry for $^3_\infty[\text{Tb(4-PyPz)}_3]$ (**9**), were carried out to investigate the thermal behavior of the two series of isotypic compounds. The DTA/TG investigations (Figures 8 and S27) reveal good temperature stability for both CPs. Except for the loss of pyridine incorporated in the pore system (signal 1) for **9** at 200°C (C$_5$H$_5$N$^+$ *m/z*

79, and C$_5$H$_4$N$^+$ *m/z* 78), both compounds show rather similar behavior in the heat flow.[29] Decomposition occurs through two consecutive endothermic processes (signal 2 and 3) with onset temperatures of 360°C and 385°C for **4** and 370°C and 405°C for **9** resulting in overall mass loss of about 42% for both. The loss of pyridine at 200°C with a corresponding mass loss of 10% in the TG-curve further confirms SCXRD data, where electron density was assigned to pyridine dispersed in the cavities of the porous 3D structure. Further confirmation for the decomposition process was the detection of a set of mass signals that can be assigned to fragments of the ligand (C$_7$H$_6$N$^+$ *m/z* 104, C$_5$H$_5$N$^+$ *m/z* 79, C$_5$H$_4$N$^+$ *m/z* 78).

## Conclusion

Ten homoleptic and luminescent trivalent lanthanide-based 3D coordination polymers with 3-(3-pyridyl)pyrazolate and 4-(4-pyridyl)pyrazolate ligands were synthesized by anhydrous solvothermal reactions and characterized by SC and PXRD, elemental analysis, IR and photoluminescence spectroscopy, and thermal analysis. The investigated compounds form two series of 3D coordination frameworks that share the overall topology of a 6-connected uninodal net with a Schläfli symbol of $4^{12}.6^3$ with **pcu** topology. Both series of frameworks show photoluminescence with intra-4f emission of the Ln$^{3+}$ ions being activated by antenna effects of the ligands leading to Ln$^{3+}$ sensitization with quantum yields of up to QY = 74% for Tb$^{3+}$. Thereby, the specific trivalent Ln-ion-based emission ranges from green via yellow to red (from Tb via Dy and Sm to Eu). Tuning of the luminescence chromaticity is further possible by co-doping of the Gd-containing frameworks of both series with Eu$^{3+}$ and Tb$^{3+}$, and allows for a chromaticity from green via yellow to red and tuning towards white-light emission.
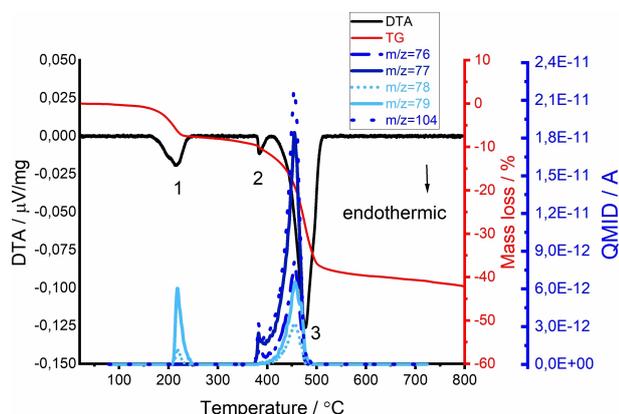


**Figure 8.** Simultaneous DTA/TG analysis together with mass spectrometry of $^{33}_\infty[\text{Tb(4-PyPz)}_3]$ (**9**) representing the series of isotypic frameworks **5–10**. Two consecutive thermal decomposition steps are numbered in the heat-flow plot. The investigation was performed under a constant flow of argon (50 mL·min$^{-1}$) with a heating from RT to 1000°C at 5 K·min$^{-1}$.

## Experimental Section

**Synthesis and analytical data**: The reactions of the different lanthanide metals with the aromatic N-heterocyclic 3-(3-pyridyl)

**Chemistry–A European Journal**

Full Paper
doi.org/10.1002/chem.202103068

**Chemistry Europe**
European Chemical
Societies Publishing

pyrazole (3-PyPzH) and 3-(4-pyridyl)pyrazole (4-PyPzH) is a redox reaction yielding hydrogen. For the two series of lanthanides ranging from Sm to Dy, the formation of trivalent compounds of the formula $^3_\infty[\text{Ln}(3\text{-PyPz})_3]$ and $^3_\infty[\text{Ln}(4\text{-PyPz})_3]$ (1–10) is observed. Detailed description of the synthesis methods for all products 1–10 and the reagents can be found in the Supporting Information.

$$\text{Ln} + C_8H_7N_3 \longrightarrow {}^3_\infty[\text{Ln}(C_8H_6N_3)_3] + {}^3/_2\,H_2$$
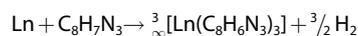
Deposition Numbers 2075974 (for 1), 2075975 (for 2), 2075976 (for 3), 2075977 (for 4), 2075978 (for 5), 2075979 (for 6), 2075980 (for 7), 2075981 (for 8), 2075982 (for 9), and 2075983 (for 10) contain the supplementary crystallographic data for this paper. These data are provided free of charge by the joint Cambridge Crystallographic Data Centre and Fachinformationszentrum Karlsruhe Access Structures service. Details on crystallographic data, comparison of simulated and recorded powder XRD patterns, detailed IR bands from ATR-MIR investigations, page size photoluminescence spectra with designated 4f–4f transitions for compounds 1–10 can be found in the Supporting Information.

## Acknowledgements

## Conflict of Interest

The authors declare no conflict of interest.

[1] a) M. F. Ashby, Y. J. M. Bréchet, *Acta Mater.* **2003**, *51*, 5801–5821; b) C. Janiak, J. K. Vieth, *New J. Chem.* **2010**, *34*, 2366–2388; c) K. Binnemans, *Chem. Rev.* **2009**, *109*, 4283–4374; d) H. Hiraga, H. Miyasaka, K. Nakata, T. Kajiwara, S. Takaishi, Y. Oshima, H. Nojiri, M. Yamashita, *Inorg. Chem.* **2007**, *46*, 9661–9671; e) X. Tan, Y.-Z. Du, Y.-X. Che, J.-M. Zheng, *Inorg. Chem. Commun.* **2013**, *36*, 63–67; f) B. Fernández, I. Oyarzabal, J. M. Seco, E. S. Sebastián, D. Fairen-Jiménez, S. Gómez-Ruiz, A. Salinas-Castillo, A. J. Calahorro, A. Rodríguez-Diéguez, *Polymer* **2016**, *8*, 39–49; g) S. R. Batten, B. Chen, J. J. Vittal, *ChemPlusChem* **2016**, *81*, 669–670; h) B. Y. Guan, A. Kushima, L. Yu, S. Li, J. Li, X. W. Lou, *Adv. Mater.* **2017**, *29*, 1605902–1605909; i) P. W. Zabierowski, O. Jeannin, T. Fix, J.-F. Guillemoles, L. J. Charbonnière, A. M. Nonat, *Inorg. Chem.* **2021**, *60*, 8304–8314; j) M. Kato, H. Ito, M. Hasegawa, K. Ishii, *Chem. Eur. J.* **2019**, *25*, 5105–5112.

[2] a) H. Furukawa, N. Ko, Y. B. Go, N. Aratani, S. B. Choi, E. Choi, A. Ö. Yazaydin, R. Q. Snurr, M. O'Keeffe, J. Kim, O. M. Yaghi, *Science* **2010**, *329*, 424–428; b) S. S. Mondal, A. Bhunia, A. G. Attallah, P. R. Matthes, A. Kelling, U. Schilde, K. Müller-Buschbaum, R. Krause-Rehberg, C. Janiak, H.-J. Holdt, *Chem. Eur. J.* **2016**, *22*, 6905–6913.

[3] a) J. Luzon, R. Sessoli, *Dalton Trans.* **2012**, *41*, 13556–13567; b) G. Cucinotta, M. Perfetti, J. Luzon, M. Etienne, P. E. Car, A. Caneschi, G.

[4] Calvez, K. Bernot, R. Sessoli, *Angew. Chem. Int. Ed.* **2012**, *51*, 1606–1610; *Angew. Chem.* **2012**, *124*, 1638–1642; c) S. Roy, A. Chakraborty, T. K. Maji, *Coord. Chem. Rev.* **2014**, *273*, 139–164.

[4] a) M. D. Allendorf, C. A. Bauer, R. K. Bhakta, R. J. T. Houk, *Chem. Soc. Rev.* **2009**, *38*, 1330–1352; b) J. Rocha, L. D. Carlos, F. A. A. Paz, D. Ananias, *Chem. Soc. Rev.* **2011**, *40*, 926–940; c) S. Sato, A. Ishii, C. Yamada, J. Kim, C. H. Song, A. Fujiwara, M. Takata, M. Hasegawa, *Polym. J.* **2015**, *47*, 195–200.

[5] a) Y. Cui, Y. Yue, G. Qian, B. Chen, *Chem. Rev.* **2012**, *112*, 1126–1162; b) J.-P. Zou, Q. Peng, Z. Wen, G.-S. Zeng, Q.-J. Xing, G.-C. Guo, *Cryst. Growth Des.* **2010**, *10*, 2613–2619; c) K. Mandel, T. Granath, T. Wehner, M. Rey, W. Stracke, N. Vogel, G. Sextl, K. Müller-Buschbaum, *ACS Nano* **2017**, *11*, 779–787.

[6] Q.-R. Wu, J.-J. Wang, H.-M. Hu, Y.-Q. Shangguan, F. Fu, M.-L. Yang, F.-X. Dong, G.-L. Xue, *Inorg. Chem. Commun.* **2011**, *14*, 484–488.

[7] a) M. Latva, H. Takalo, V.-M. Mukkala, C. Matachescu, J. C. Rodríguez-Ubis, J. Kankare, *J. Lumin.* **1997**, *75*, 149–169; b) L. Armelao, S. Quici, F. Barigelletti, G. Accorsi, G. Bottaro, M. Cavazzini, E. Tondello, *Coord. Chem. Rev.* **2010**, *254*, 487–505; c) A. Bellusci, G. Barberio, A. Crispini, M. Ghedini, M. La Deda, D. Pucci, *Inorg. Chem.* **2005**, *44*, 1818–1825.

[8] a) H. Zhang, R. Fan, W. Chen, X. Zheng, K. Li, P. Wang, Y. Yang, *J. Lumin.* **2013**, *143*, 611–618; b) T. Wehner, K. Mandel, M. Schneider, G. Sextl, K. Müller-Buschbaum, *ACS Appl. Mater. Interfaces* **2016**, *8*, 5445–5452.

[9] a) M. B. Coban, A. Amjad, M. Aygun, H. Kara, *Inorg. Chim. Acta* **2017**, *455*, 25–33; b) C. J. Höller, P. R. Matthes, M. Adlung, C. Wickleder, K. Müller-Buschbaum, *Eur. J. Inorg. Chem.* **2012**, *3*, 5479–5484.

[10] H. Zhang, X. Shan, L. Zhou, P. Lin, R. Li, E. Ma, X. Guo, S. Du, *J. Mater. Chem. C* **2013**, *1*, 888–891.

[11] a) H. Adams, S. R. Batten, G. M. Davies, M. B. Duriska, J. C. Jeffery, P. Jensen, J. Lu, G. R. Motson, S. J. Coles, M. B. Hursthouse, M. D. Ward, *Dalton Trans.* **2005**, 1910–1923; b) J.-C. Li, H.-X. Li, H.-Y. Li, W.-J. Gong, J.-P. Lang, *Cryst. Growth Des.* **2016**, *16*, 1617–1625.

[12] F. L. Liu, J. Tao, *Chem. Eur. J.* **2017**, *23*, 18252–18257.

[13] N. Li, B. Mu, X. Cao, R. Huang, *J. Solid State Chem.* **2014**, *217*, 180–186.

[14] W. J. Gee, S. R. Batten, *Chem. Commun.* **2012**, *48*, 4830–4832.

[15] L.-R. Xing, Z. Lu, M. Li, J. Zheng, D. Li, *J. Phys. Chem. Lett.* **2020**, *11*, 2067–2073.

[16] K. Müller-Buschbaum, Y. Mokaddem, *Chem. Commun.* **2006**, 2060–2062.

[17] a) M. O'Keeffe, M. A. Peskov, S. J. Ramsden, O. M. Yaghi, *Acc. Chem. Res.* **2008**, *41*, 1782–1789; b) A. F. Wells, *Three Dimensional Nets and Polyhedra*, Wiley, New York, **1977**.

[18] N. Du, X. Gao, J. Song, Z.-N. Wang, Y.-H. Xing, F.-Y. Bai, Z. Shi, *RSC Adv.* **2016**, *6*, 71012–71024.

[19] J. H. Van Vleck, *J. Phys. Chem.* **1937**, *41*, 67–80.

[20] K. Binnemans, C. Görller-Walrand, *J. Rare Earth* **1996**, *14*, 173–180.

[21] a) K. Binnemans, *Coord. Chem. Rev.* **2015**, *295*, 1–45; b) W. T. Carnall, P. R. Fields, K. Rajnak, *J. Chem. Phys.* **1968**, *49*, 4424–4442; c) A. E. Sedykh, D. G. Kurth, K. Müller-Buschbaum, *Eur. J. Inorg. Chem.* **2019**, *2019*, 4564–4571.

[22] A. E. Sedykh, D. G. Kurth, K. Müller-Buschbaum, *Z. Anorg. Allg. Chem.* **2021**, *647*, 359–364.

[23] P. R. Matthes, C. J. Höller, M. Mai, J. Heck, S. J. Sedlmaier, S. Schmiechen, C. Feldmann, W. Schnick, K. Müller-Buschbaum, *J. Mater. Chem.* **2012**, *22*, 10179–10187.

[24] a) A. P. Bassett, S. W. Magennis, P. B. Glover, D. J. Lewis, N. Spencer, S. Parsons, R. M. Williams, L. De Cola, Z. Pikramenou, *J. Am. Chem. Soc.* **2004**, *126*, 9413–9424; b) X. Y. Chen, M. P. Jensen, G. K. Liu, *J. Phys. Chem. B* **2005**, *109*, 13991–13999; c) J. M. Stanley, C. K. Chan, X. Yang, R. A. Jones, B. J. Holliday, *Polyhedron* **2010**, *29*, 2511–2515.

[25] H. Hakala, P. Liitti, J. Peuralahti, J. Karvinen, V.-M. Mukkala, J. Hovinen, *J. Lumin.* **2005**, *113*, 17–26.

[26] A. K. Mondal, S. Goswami, S. Konar, *Dalton Trans.* **2015**, *44*, 5086–5094.

[27] a) A. Aebischer, F. Gumy, J.-C. G. Bünzli, *Phys. Chem. Chem. Phys.* **2009**, *11*, 1346–1353; b) M. H. V. Werts, R. T. F. Jukes, J. W. Verhoeven, *Phys. Chem. Chem. Phys.* **2002**, *4*, 1542–1548.

[28] S. V. Eliseeva, J.-C. G. Bünzli, *Chem. Soc. Rev.* **2010**, *39*, 189–227.

[29] K. Müller-Buschbaum, C. C. Quitmann, *Inorg. Chem.* **2006**, *45*, 2678–2687.